Institute of Remote Sensing and Digital Earth
Chinese Academy of Sciences

cal con
Conference on Characterization and
Radiometric Calibration for Remote Sensing

A Method Suitable for Vicarious Calibration of a UAV Hyperspectral Remote Sensor

Hao Zhang[1], Haiwei Li[1], Benyong Yang[2], Zhengchao Chen[1]

1. Institute of Remote Sensing and Digital Earth (RADI), Chinese Academy of Sciences (CAS)
2. Hefei Institutes of Physical Science, CAS

Outline

1. Background
2. Method
3. Experiment and Result
4. Discussion
5. Summary

1. Backgrounds

Many applications from UAV:

- agriculture, forest, water, disaster monitoring, environment protection

The necessary of vicarious calibration for UAV's:

- The conditions of vicarious calibration are real ones
- Vicarious calibration results are valuable supplements to the laboratory's
- UAV's sensor is vulnerable to vibrations and wind current

2.Method

Vicarious Calibration:

The reflectance-based method

- Ground reflectance, AOD, water vapor abundance
- Widely used in vicarious calibration
- mostly used to calibrate airborne sensors in the case of highly visibility (low aerosol burden), like AVIRIS, HYDICE, Hymap

The irradiance-based method

- + diffuse-to-global irradiance ratios
- Reduce the uncertainty caused by aerosol type assumption

2.Method

Improvement :

For satellite sensor

For UAV sensor

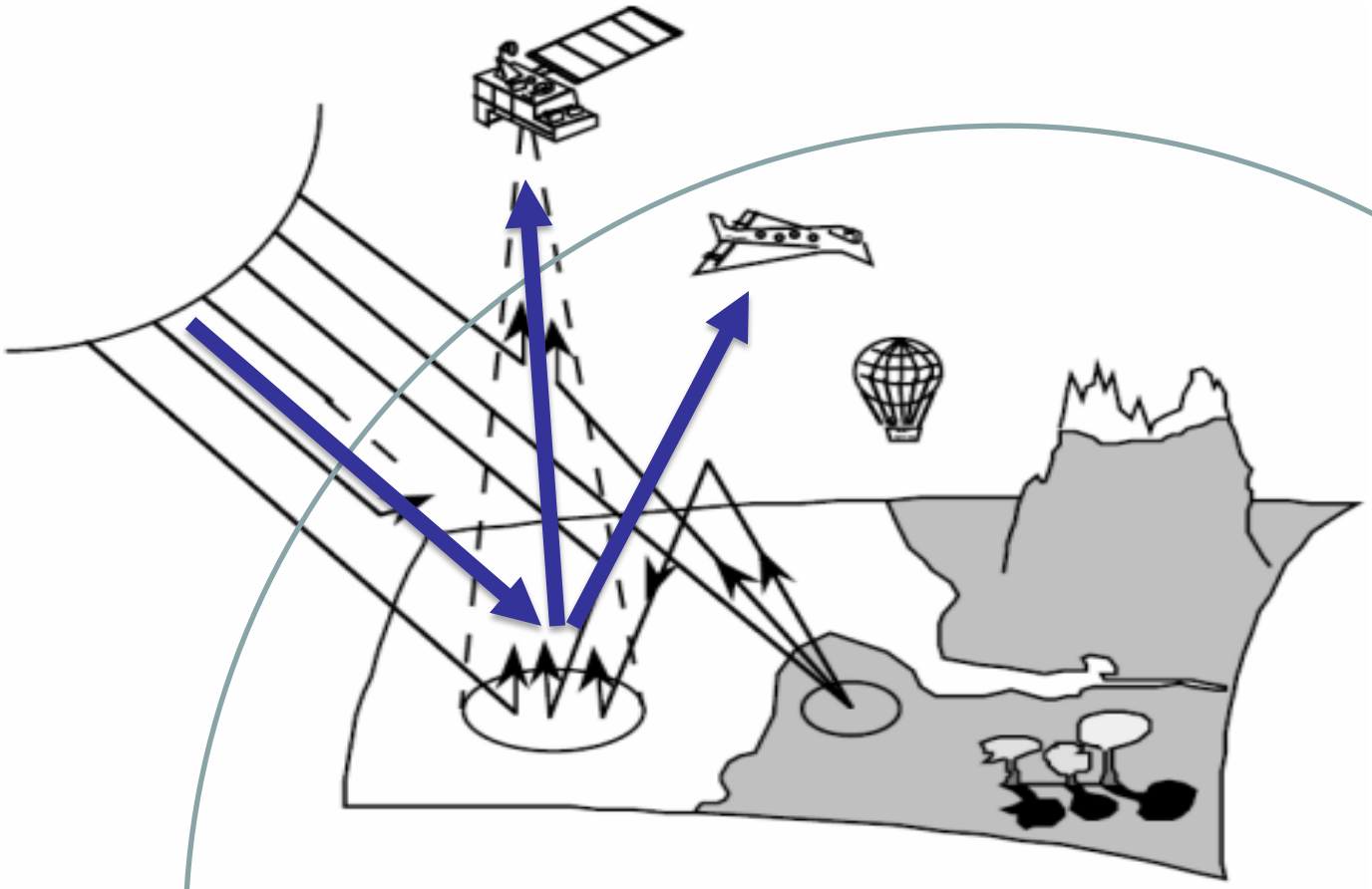

2. Method

Improvement :

Irradiance-based method use for satellite sensor

The total transmittance of solar path and view path

$$\rho^*(\theta_s,\theta_v,\phi_{v-s}) = \rho_a(\theta_s,\theta_v,\phi_{v-s}) + \frac{\rho_t}{1-s\cdot\rho_t}\cdot T(\theta_s)\cdot T(\theta_v)$$

ρ^*: TOA reflectance

ρ_a: Molecular and aerosol contribution

ρ_t: Atmospheric albedo

$$T(\theta_v) = \frac{(1-\rho s)e^{-\delta/\mu_v}}{1-\alpha_v}$$

$$T(\theta_s) = \frac{(1-\rho s)e^{-\delta/\mu_s}}{1-\alpha_s}$$

$$\rho^* = \rho_a + \frac{e^{-\delta/\mu_s}}{1-\alpha_s}\cdot\rho(1-\rho s)\cdot\frac{e^{-\delta/\mu_v}}{1-\alpha_v}$$

Irradiance-based method use for UAV sensor

$$\rho^* = \rho_a + \frac{\rho}{1-\rho S}\cdot\frac{(1-\rho_c S)e^{-\delta/\mu_s}}{1-\alpha_s}\cdot T(\theta_v)$$

- Only the total transmittance in the solar direction was substituted,
- The total transmittance in the view path was not change.

3. Experiments and Results

RTM Simulation:

Apparent reflectance difference due to aerosol type assumptions

- ✓ $diff. = 1 - \frac{\rho^*(urban\ aerosol)}{\rho^*(rural\ aerosol)}$
- ✓ diff. changes with AOT & UAV's height
- ✓ Reflectance-based method
- ✓ Irradiance-based method

diffuse-to-global ratios were computed under the rural aerosol assumption

Para.	Value
Atmosphere model	MLS
CO_2	360ppmv
H_2O	0.776 g/cm^2
Ozone column density	0.315atm-cm
Solar zenith	44.02°
Viewing zenith	0°
Relative azimuth	90°
AOT@550nm	0.05, 0.1, 0.5
Heights (km)	0.2, 1.0 and 5.0
Ground Refl.	0.6

3. Experiments and Results

- RTM Simulation:

Relative difference = (urban. / rural. -1) * 100%

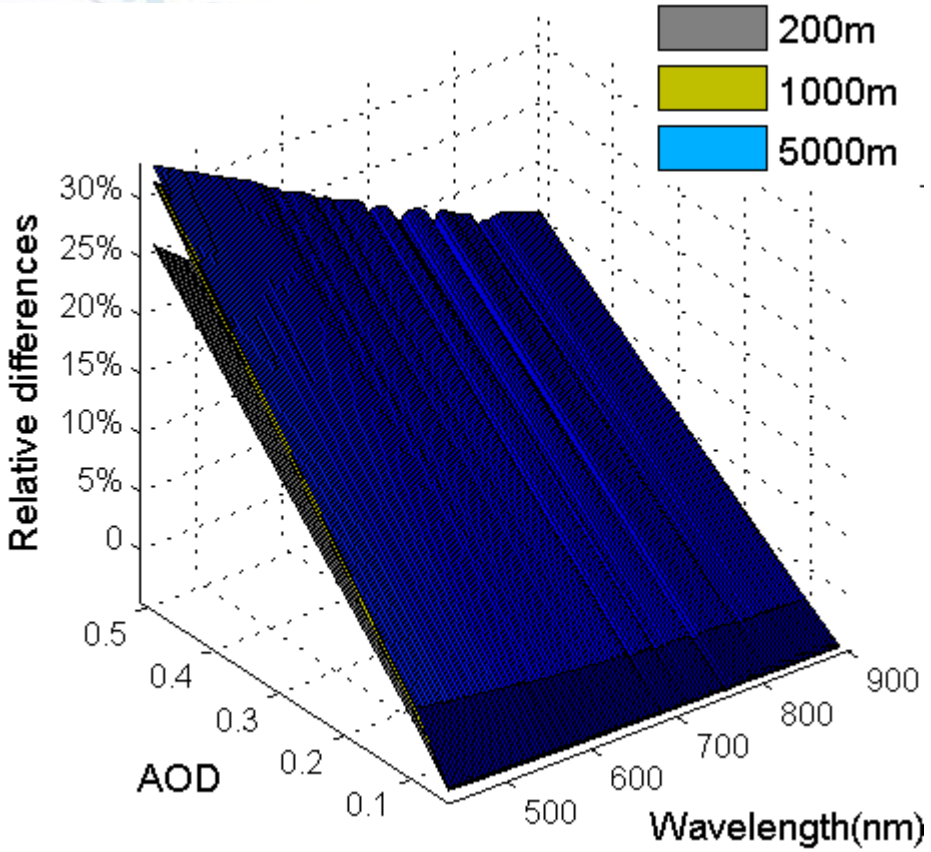

the reflectance-based method

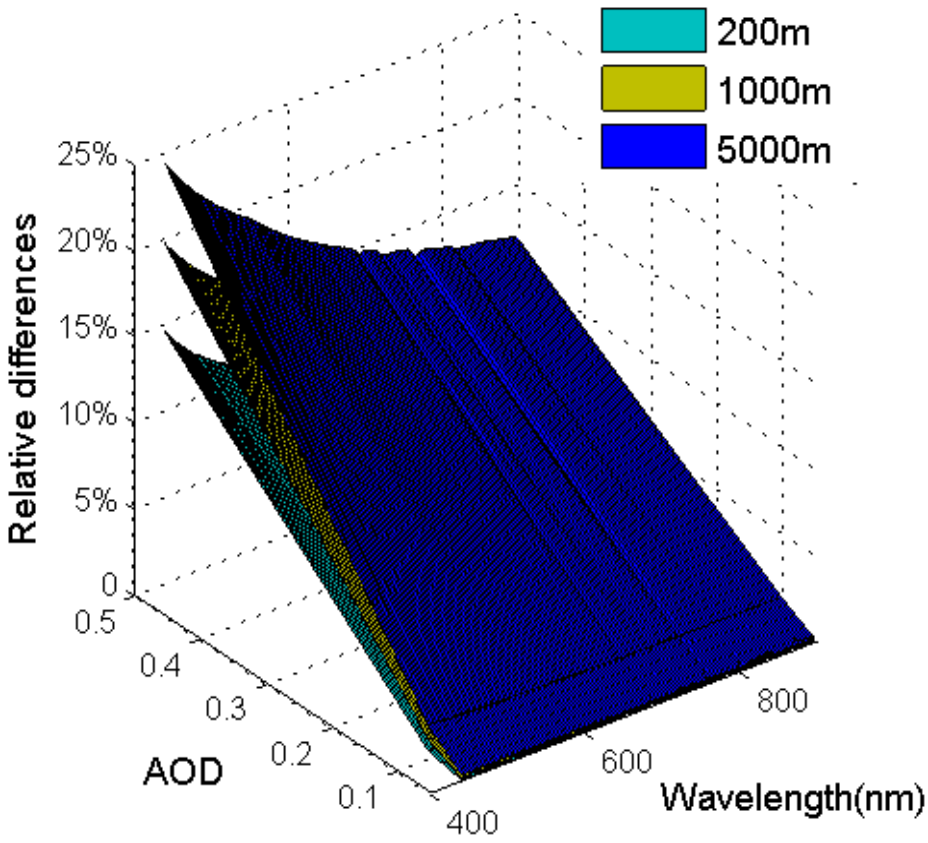

the improved irradiance-based method

3. Experiments and Results

RTM Simulation:

The average relative differences between two aerosol types for each case of all bands

-- **AOD (0.55um)**	reflectance-based method (%)			Improved method (%)		
	5000m	1000m	200m	5000m	1000m	200m
AOD 0.05	0.79	0.68	0.57	0.29	0.19	0.1
AOD 0.1	4.06	3.48	2.93	1.57	1.03	0.56
AOD 0.5	28.78	26.09	21.72	16.32	12.92	8.94

- The improved method has lower uncertainty
- The advantage is more evident with height and AOD

3. Experiments and Results

- Field Experiment I: fair weather

- On the Sept 25th, 2013
- The civilian airport of Suizhong in the Chinese province of Liaoning.
  (40.23N, 120.21E)
- Runway

Long: 200m Wide:12m

3. Experiments and Results

Headwall's Micro-Hyperspec	
Wavelength Range(nm)	380-1000nm
Spectral Resolution (nm)	<10nm
Spectral Bands	125
The most spectral line bending	0.1%
The biggest trapezoidal distortion	0.1%
Focal Length	17.0mm
Weight (without lens)	0.9kg
Height	1300m

Hyperspectral UAV(Integrated by Goldwn way Scientific, Inc. China,www.goldway.com.cn)

3. Experiments and Results

The measurement of ground spectrum :

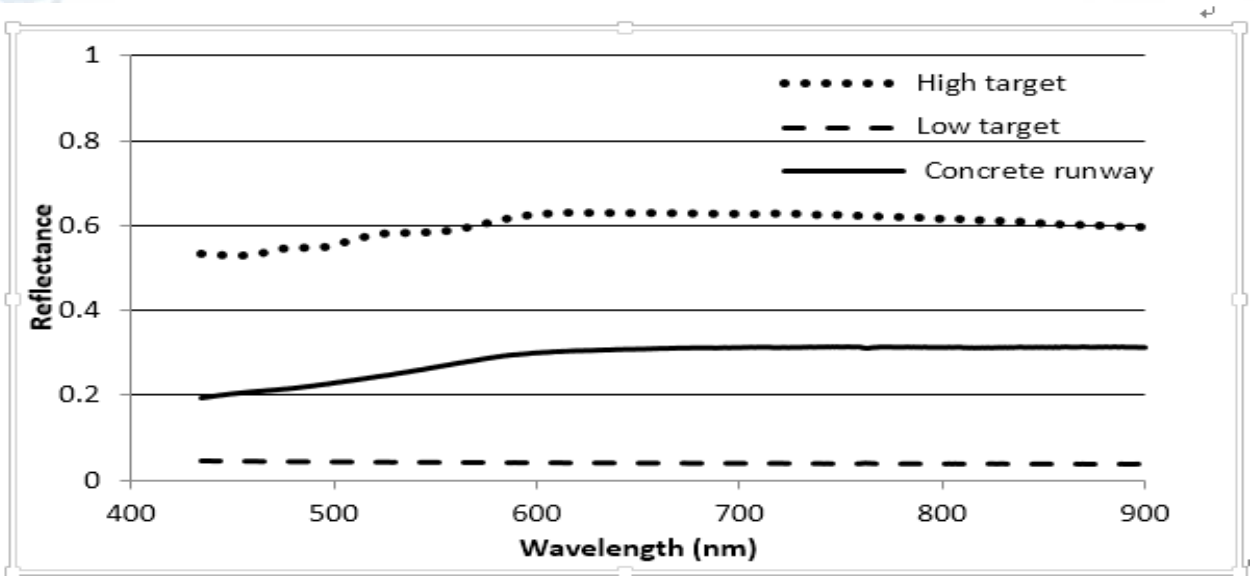

Surface Reflectance

ASD

Tarp: reflectance of 60%

Tarp: reflectance of 5%

Cement runway

3. Experiments and Results

The measurement of atmospheric characteristics :

CE318

barometer

Diffuse-to-global irradiance ratios

AOT@550 nm	**0.052**
H2O(g/cm^2)	0.776
Aerosol Type	Rural
Atmospheric Model	MLS
Ozone density (cm-atm)	0.310

3. Experiments and Results

Image Pre-Processing:

Raw image

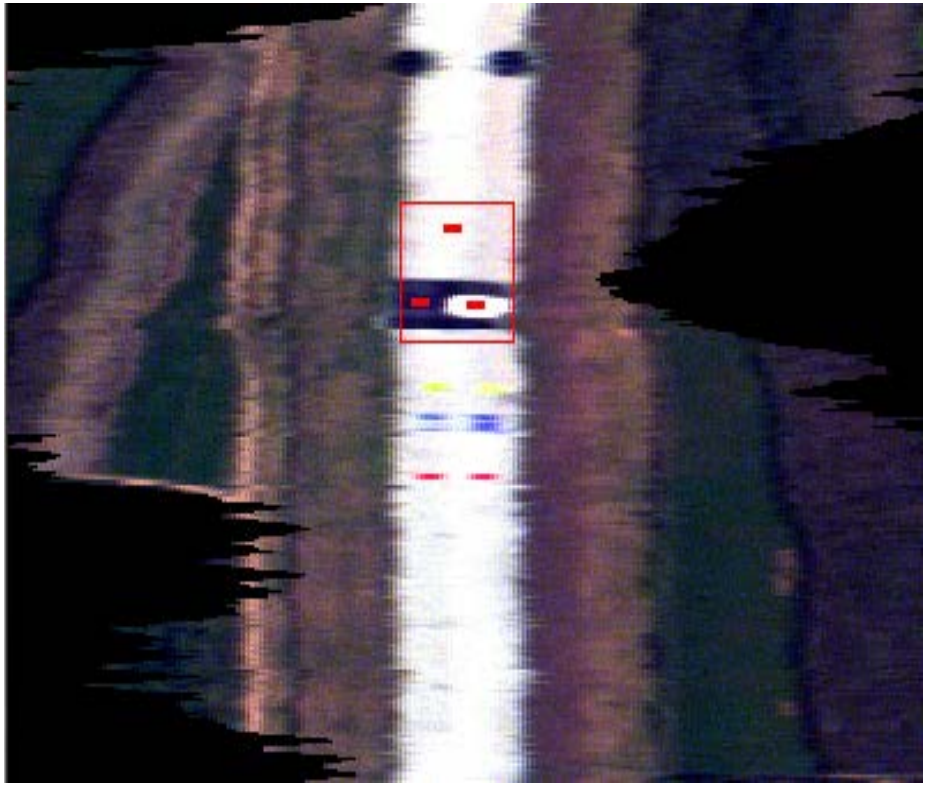

Geo-rectification

3. Experiments and Results

Calibration_coefficients_:

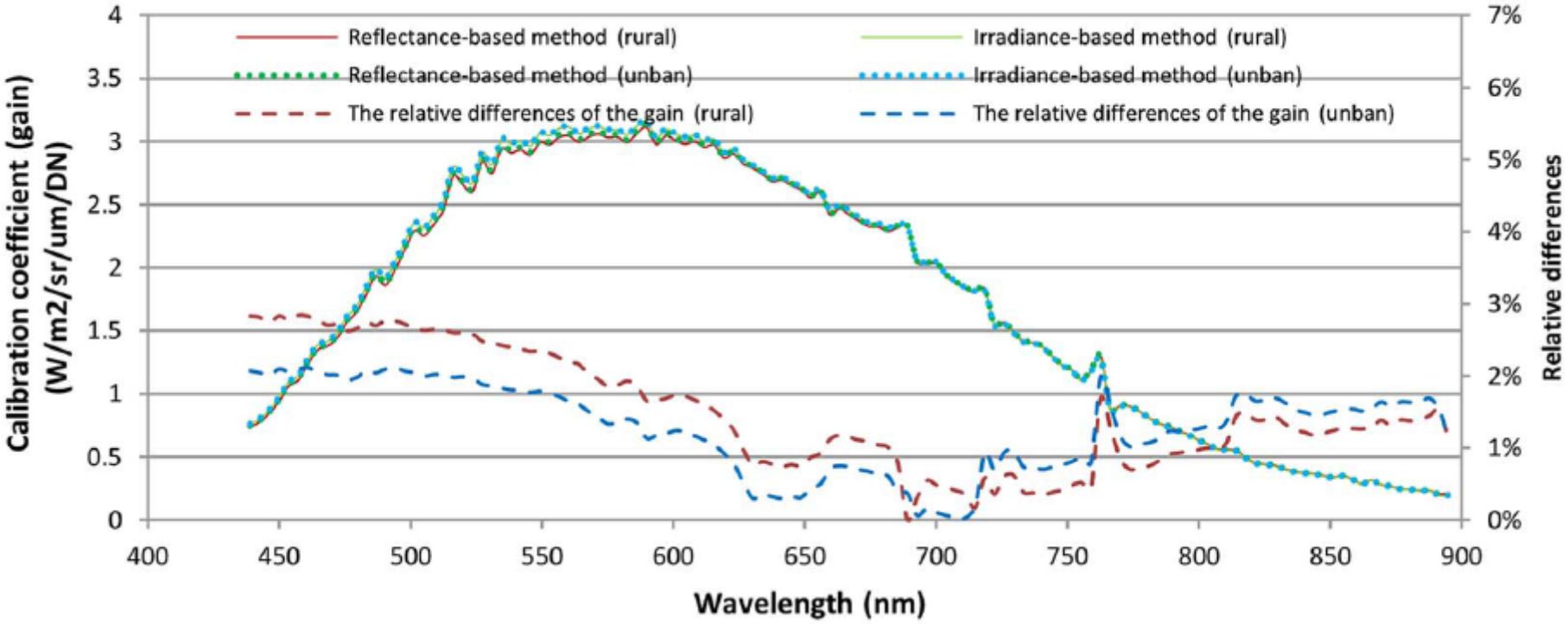

The calibration coefficients (gain) for the reflectance-based and the irradiance-based methods and their relative difference

3. Experiments and Results

The radiances of the runway cement:

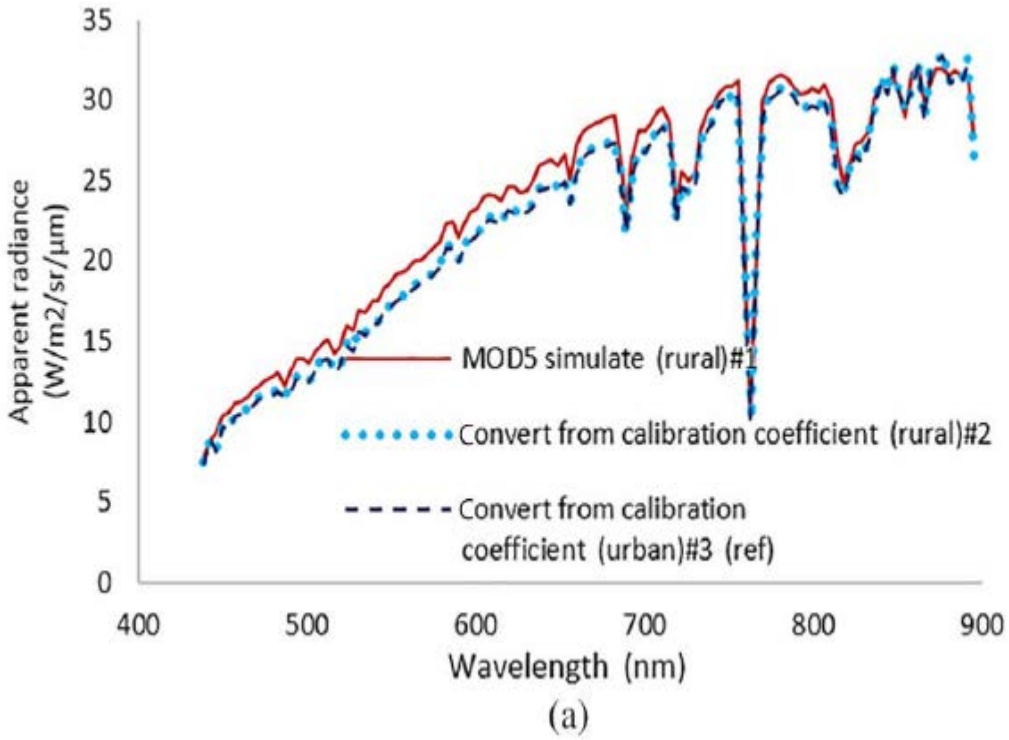

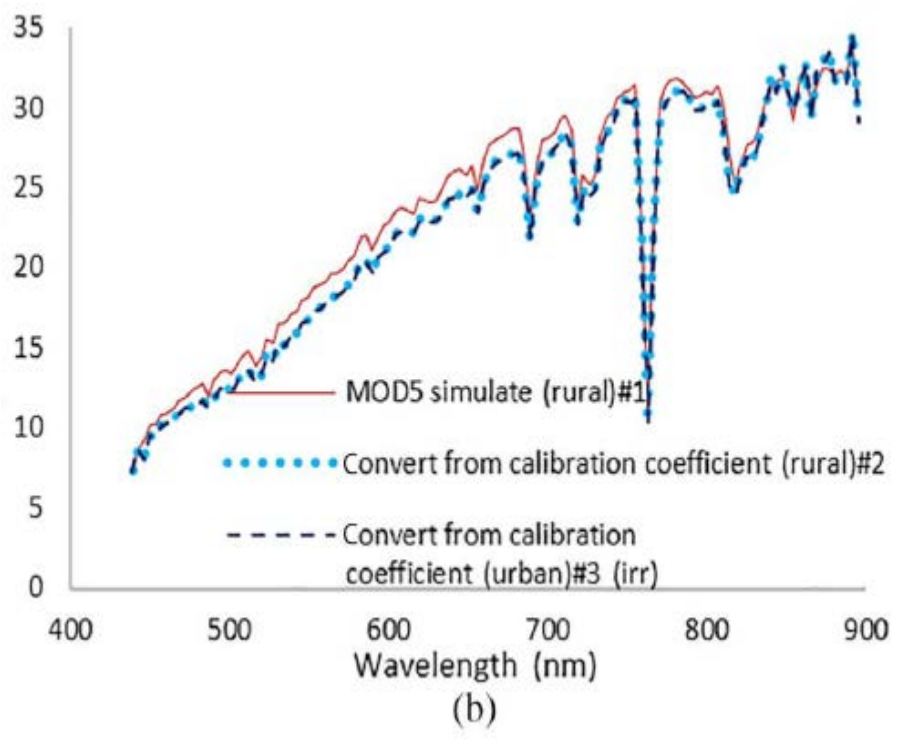

(a) Comparison of results from reflectance-based method

(b) Comparison of results from irradiance-based method

3. Experiments and Results

The different wavelength ranges:

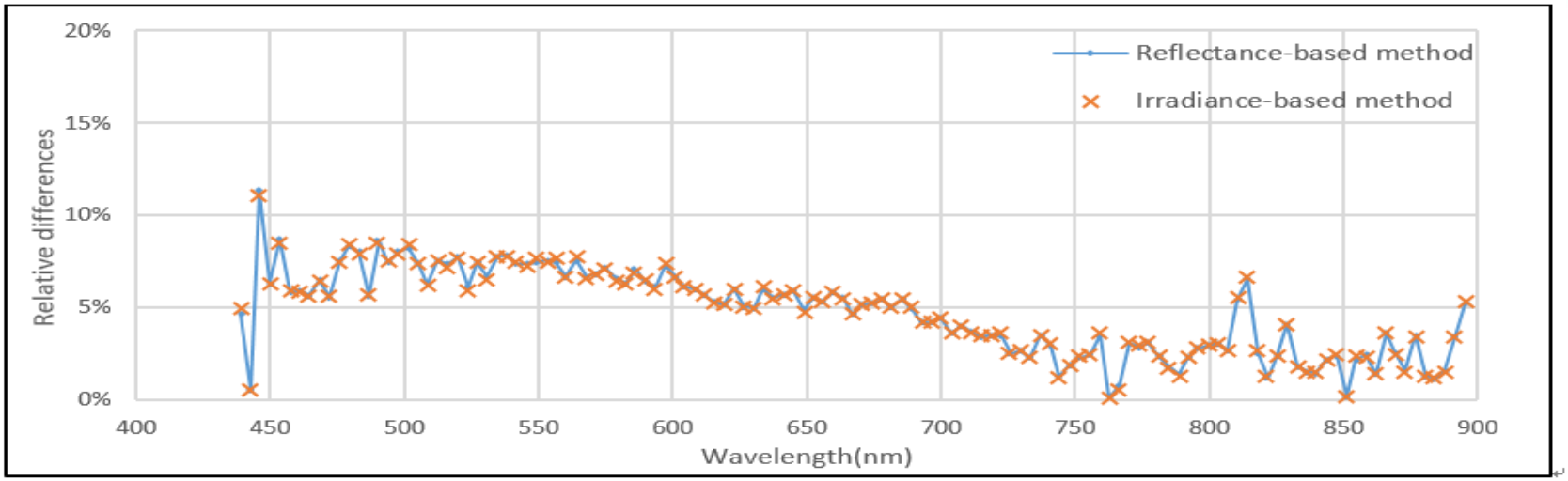

The relative differences for the reflectance-based and the irradiance-based method

The average relative differences**(Imagery /MOD5 -1**) wavelength ranges

Band	Wavelength range (nm)	Average for the reflectance-based method (#1–#2) (%)	Average for the irradiance-based method (#1–#2) (%)	Average for the reflectance-based method (#1–#3) (%)	Average for the irradiance-based method (#1–#3) (%)
c. 1–7	c. 400–500	6.80	6.70	7.68	7.05
c. 18–58	c. 501–650	6.55	6.58	7.39	6.89
c. 60–125	c. 651–900	3.09	3.10	3.47	3.27
–	Total bands	4.73	4.73	5.34	4.97

3. Experiments and Results

- Field Experiment II: unIdeal weather

- On June 28th, 2014
- Aviation School of Baoding, Hebei, China (38.87N, 115.33E)
- Headwall's Micro-Hyperspectral airborne sensor: 377-972nm (162bands)
- Flight: 120m

3. Experiments and Results

In-situ measurements and images

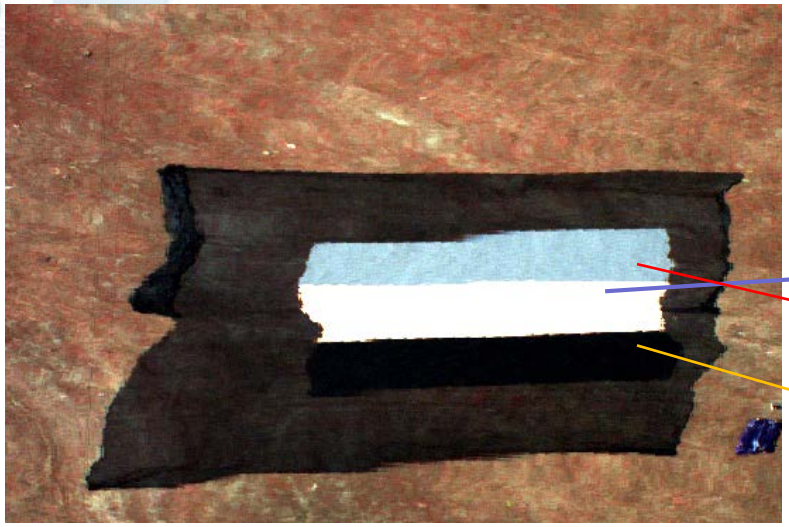

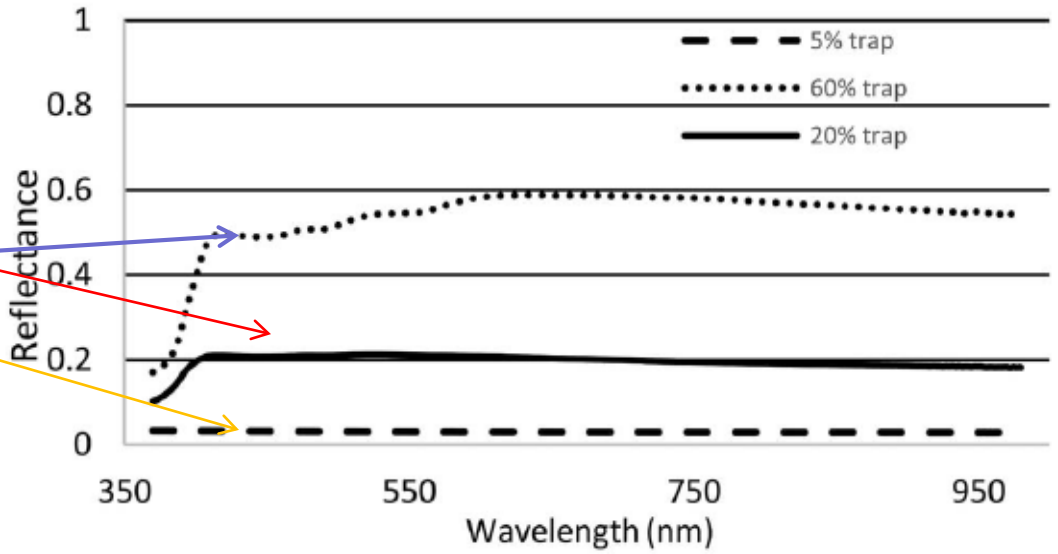

AOT@550 nm	**0.54**
H2O(g/cm^2)	1.6
Aerosol Type	Rural
Atmospheric Model	MLS
Ozone density	0.315

3. Experiments and Results

The radiances of the gray tarp (20%)

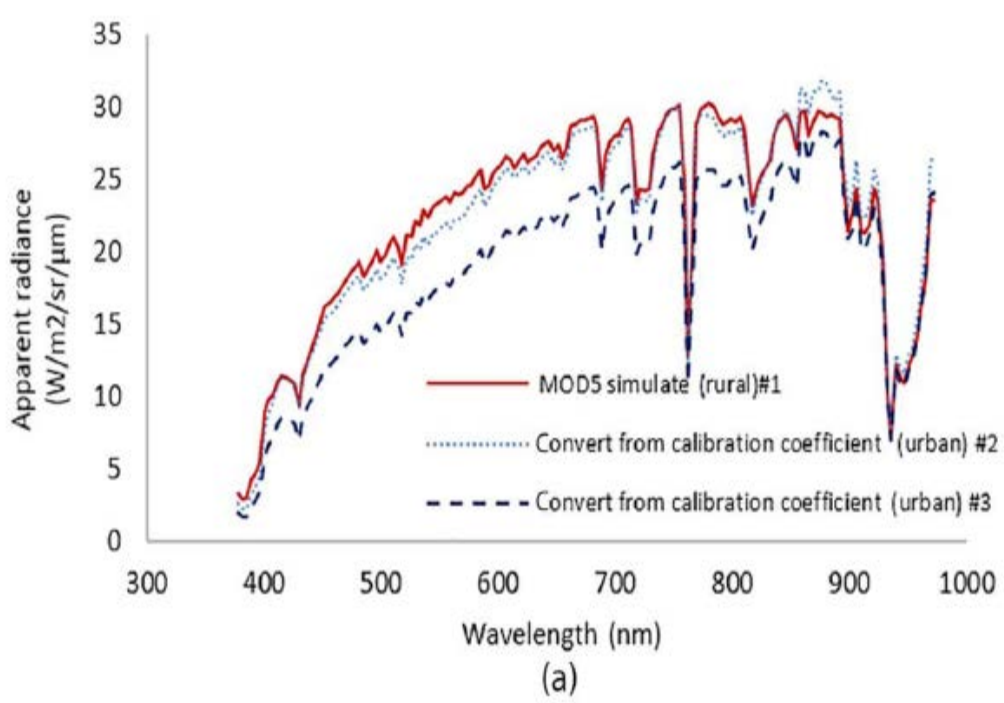

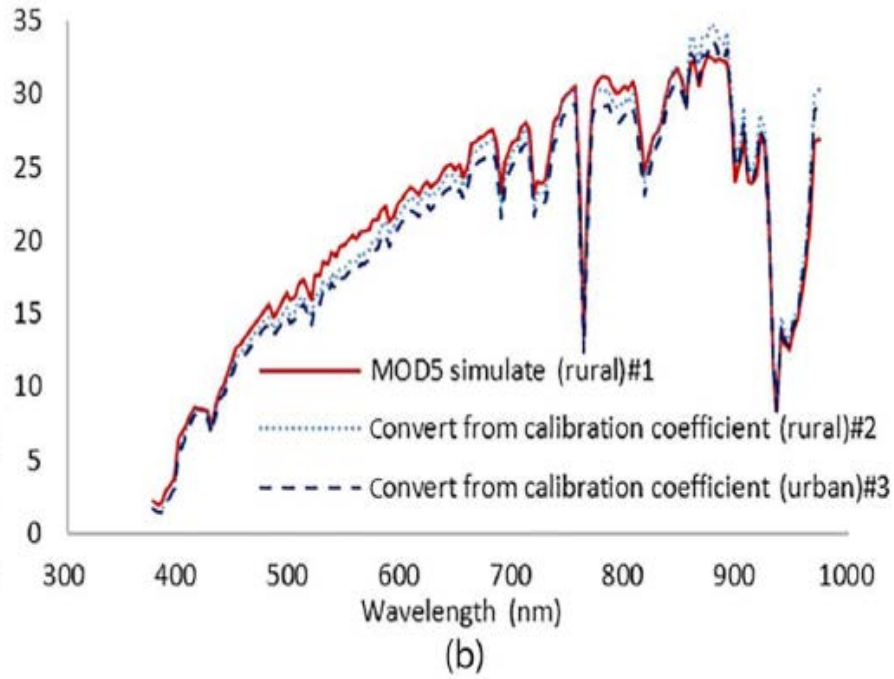

(a) Comparison of results from reflectance-based method

(b) Comparison of results from irradiance-based method

3. Experiments and Results

The relative differences for the reflectance-based and the irradiance-based method

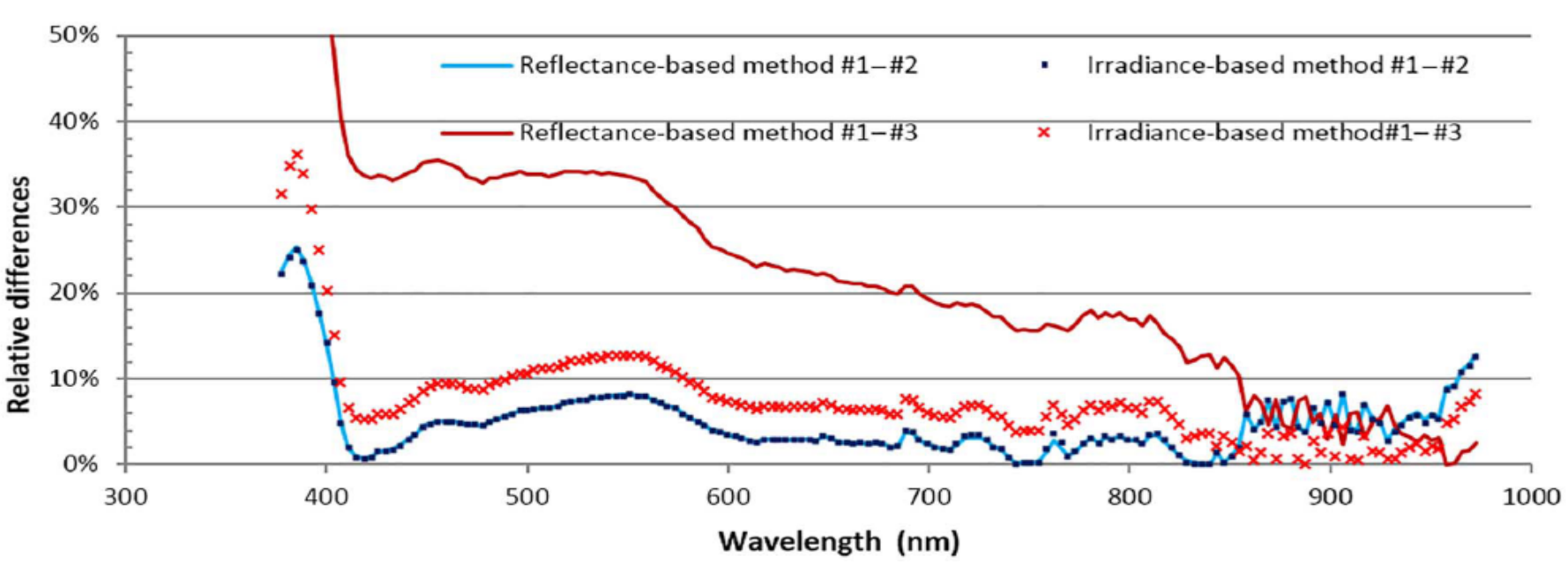

Band	Wavelength range (nm)	Average for the reflectance-based method (#1–#2) (%)	Average for the irradiance-based method (#1–#2) (%)	Average for the reflectance-based method (#1–#3) (%)	Average for the irradiance-based method (#1–#3) (%)
c. 1–13	c. 400–500	12.96	12.80	54.6	19.9
c. 14–149	c. 501–650	3.91	3.91	21.53	6.77
c. 150–162	c. 651–900	7.24	6.98	2.79	3.46
–	All bands	4.90	4.88	22.68	7.55

4. Discussion

- Uncertainty due to aerosol type assumption

The average relative differences for the different experiments

	Field experiment Ⅰ (Suizhong)		**Field experiment Ⅱ (Baoding)**	
	Rural and maritime	Rural and urban	Rural and maritime	Rural and urban
Reflectance -based method	0.4%	0.68%	15.75%	18.69%
Improved irradiance-based method	0.25%	0.23	3.49%	8.01%

4. Discussion

- Uncertainty v.s. AOT

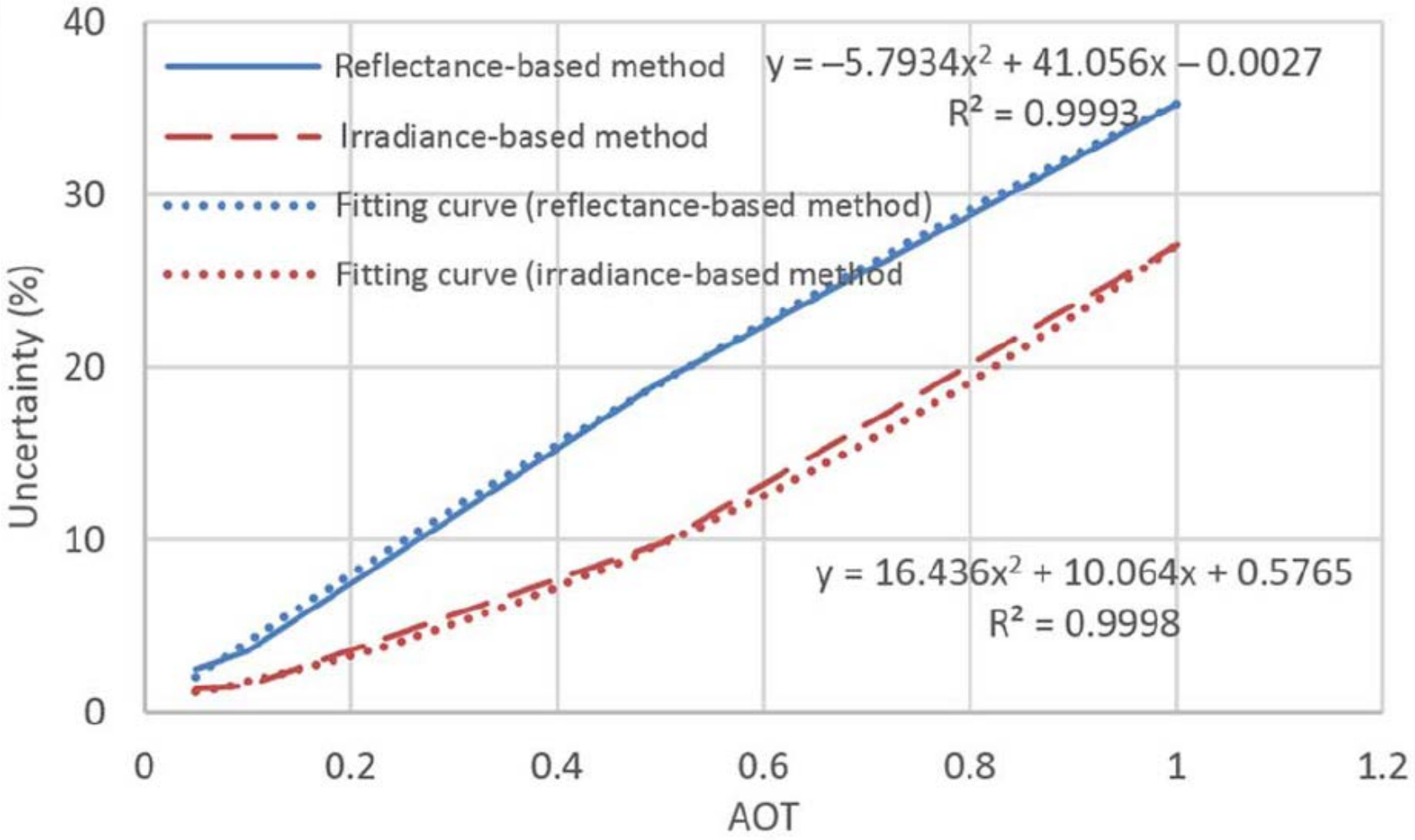

5. Conclusion

- We present an improved irradiance-based method which consider the different imaging paths between airborne RS and satellite RS.

- Two typical experiments with lower and higher aerosol burden were carried out and validated our new method.

- The improved irradiance-based method is more suitable for UAV sensor vicarious calibration and is more accuarate

Thanks!

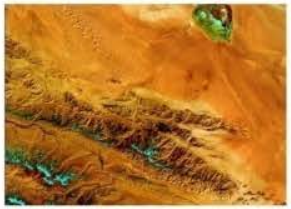




Institute of Remote Sensing and Digital Earth
Chinese Academy of Sciences

Add：No.9 Dengzhuang South Road,Haidian District,Beijing 100094,China
Tel：86-10-82178008 Fax：86-10-82178009
E-mail：office@radi.ac.cn
Web：www.radi.cas.cn